Systematics of *f*-element crystal-field interaction

G.K. Liu*

Chemistry Division, Argonne National Laboratory, 9700 South Cass Avenue, Argonne (Lemont), IL 60439, USA

Abstract

Systematic behaviors of free-ion and crystal-field interactions are elucidated as a function of N, the number of f electrons in a lanthanide or actinide ion. Experimentally determined values of the free-ion interaction parameters are compared with those calculated based on Hartree-Fock theory. Comparison is also made between the lanthanide series in $4f^N$ configurations and the actinide series in $5f^N$ configurations. Variation in intra-ionic electrostatic interaction, spin–orbit coupling, and ion–ligand interaction is analyzed in comparison between the iso-f-electron lanthanide and actinide ions. Based on an exchange-charge model of crystal-field theory, crystal-field parameters of the f-element ions in various crystals are summarized in terms of point charge contribution and covalence effect. A systematic correlation is found between the free-ion parameters and the crystal-field strength. Increase of the crystal-field interaction results in a reduction in the free-ion parameters.
© 2004 Elsevier Inc. All rights reserved.

Keywords: *f*-element spectroscopy; Ion–ligand interaction; Crystal-field theory

1. Introduction

Because of similarities in the electronic property of the lanthanide series in $4f^N$ configurations and that of the actinide series in $5f^N$, the electronic transitions and optical spectra of the *f*-element ions in these two series in solids exhibit the same systematic behaviors. The fundamental spectroscopic properties of the *f*-element ions have been interpreted using a common framework of crystal-field theory [1–9]. The well-developed theoretical framework for modeling the electronic interactions and analyzing the optical spectra of lanthanide ions has been adapted successfully to modeling the actinides as well [10–18].

The systematic behaviors of the *f*-element ions are established through parameterization of an effective operator Hamiltonian including various terms of free-ion interaction and crystal-field interaction

$$\mathscr{H} = \mathscr{H}_{FI} + \mathscr{H}_{CF}. \tag{1}$$

The parameterization is achieved through fitting of the observed energy levels of the *f*-element ions in crystalline lattice while the Hamiltonian is diagnolized in the intermediate coupling scheme. Specifically, the free-ion interaction in Eq. (1) is defined as [5,15]

$$\begin{aligned}
\mathscr{H}_{FI} &= \sum_{k=0,2,4,6} F^k f_k + \zeta_{nl} A_{SO}(nl) \\
&\quad + \alpha L(L+1) + \beta G(G_2) + \gamma G(R_7) \\
&\quad + \sum_{i=2,3,4,6,7,8} T^i t_i + \sum_{i=0,2,4} M^i m_i + \sum_{i=2,4,6} p_i P^i. \tag{2}
\end{aligned}$$

The physical nature of the parameters associated with the free-ion operators is that F^k are the slater radial integrals for the radial part of the electrostatic interaction; ζ_{nl} the spin–orbit interaction; α, β, γ the effective configuration interaction evaluated with angular momentum operator L and Casimir operators G_2 and R_7 [19]; T^i the three-particle coupling [20–22]; M^i the relativistic effects including spin–spin and spin-other-orbit coupling [23]; and P^i the effective two-body interaction introduced to account for configuration

*Fax: +630 252 7501.

E-mail address: gkliu@anl.gov (G.K. Liu).

interaction through electrostatically correlated magnetic interactions [23,24].

Following Wybourne's formalism [1], the crystal-field potential may be defined by:

$$\mathscr{H}_{CF} = \sum_{k,q,i} B_q^k C_q^{(k)}(i), \tag{3}$$

where the summation involving i is over all N electrons of the ion of interest; B_q^k are crystal-field parameters and $C_q^{(k)}$ are components of tensor operators that transform like spherical harmonics.

The interplay of experimental investigation and theoretical development was essential to make the crystal field modeling a great success. For more than three decades, Carnall and his coworkers have accomplished remarkably in developing the procedures for modeling the f-element spectra. From systematic analysis of the spectra of trivalent lanthanide ions (Ln^{3+}) in LaCl$_3$ in 1960s [4,25,26] and the similar work on Ln^{3+}:LaF$_3$ in 1970s [5–7] to systematic studies of trivalent actinide ions (An^{3+}) in LaCl$_3$ [11,27,28] and tetravalent actinide ions (An^{4+}) in the 1980s and 1990s [10,12,16], the empirical approach has become a standard procedure in modeling f-element electronic structure and spectroscopic properties.

A systematic interpretation of trivalent actinide and lanthanide spectra was initially developed through a linear extrapolation based on the fitted parameters that were available from the analyses of the optical spectra of other individual ions. As more extensive data and improved modeling yielded better determined and more consistent F^k and ζ_{nf} values for the trivalent lanthanides and actinides, it became apparent that the variation in the parameters was non-linear [5,11]. This non-linearity could also be observed in the values of parameters of the ab initio calculations using Hartree-Fock (HF) method [7]. The difference between the HF values and fitted values of parameters (ΔF and $\Delta\zeta$) appears to exhibit a much more linear variation with N than the parameter values themselves. Consequently, the difference has been adopted as the basis for a useful predictive model.

Evaluation of ion–ligand interaction and crystal-field energy level structure is theoretically much more difficult than predicting the number of energy levels for each free-ion state. The empirical model of free-ion and crystal-field interaction is by no means perfect. Various interaction mechanisms that influence the electronic states of a lanthanide or actinide ion in a solid environment may not be accurately determined in the framework of crystal field modeling. However, the empirical approach is currently the most effective method for evaluation of the spectroscopic properties of f-element ions in solids [11,16,17].

Phenomenological modeling and ab initio calculations of ion–ligand interactions are able to provide theoretical guidance to analysis of crystal field spectra.

From theoretical approaches, analytical expressions of crystal field parameters using phenomenological models are available for calculating the crystal-field parameters of actinide and lanthanide ions in a specific crystalline lattice. The exchange charge model (ECM) [29,30] and the superposition model [31,32] are two crystal field models that have achieved significant success and are useful for guiding spectral analyses. In addition, ab initio calculations of the solid-state electronic energy level structure have advanced significantly along with the rapid development of computer technology and are likely to be increasingly important in future studies [33,34].

Understanding the electronic properties of f-element ions and their systematic behaviors is essential for interpreting the optical spectra and excited state dynamics of these ions in condensed phases. In this paper, we present an overall review of the systematic trends in the f-element spectroscopic properties. A comparison is made between the lanthanides and actinides. Several important results from systematic analyses of f-element crystal-field spectra are discussed in more detail.

2. A comparison between lanthanides and actinides

2.1. Systematic trends in free-ion interaction

The most important trends are those of the electrostatic-interaction parameters F^k and spin–orbit parameter ζ_{nf} which increase with the number of f-electrons, N. This increase reflects the consequence of changes in the f-electron orbital and electronic interaction. The experimentally determined values of F^2 and ζ_{nf} for trivalent lanthanide in LaF$_3$, trivalent actinide in LaCl$_3$, and tetravalent actinide in AnF$_4$ are shown as a function of N in Figs. 1 and 2, respectively [5,11,16]. The experimental values are plotted in comparison with the relativistic Hartree-Fock (HFR) values. Detailed results of HFR calculations on f-electrons were previously discussed by Crosswhite and Crosswhite [35] and Carnall et al. [36]. Although the HFR calculations predict the same trends across the series, the HFR values for F^k and ζ_{nf} are always larger than the empirical parameters obtained by allowing them to vary in fitting experimental data. The HFR values [7] plotted in Figs. 1 and 2 are normalized to the fitted values for the f^2 or f^3 ion. The HFR values of ζ_{nf} agree remarkably well with empirical values, while the F^k values remain considerably larger than the empirical values. Presumably, this is because, in addition to relativistic effects, f-electron coupling with orbitals of higher-lying energies reduces the radial integrals assumed in the HFR approximation. Moreover, the experimental results are obtained for ions in condensed phases, not in a gaseous phase, which leads
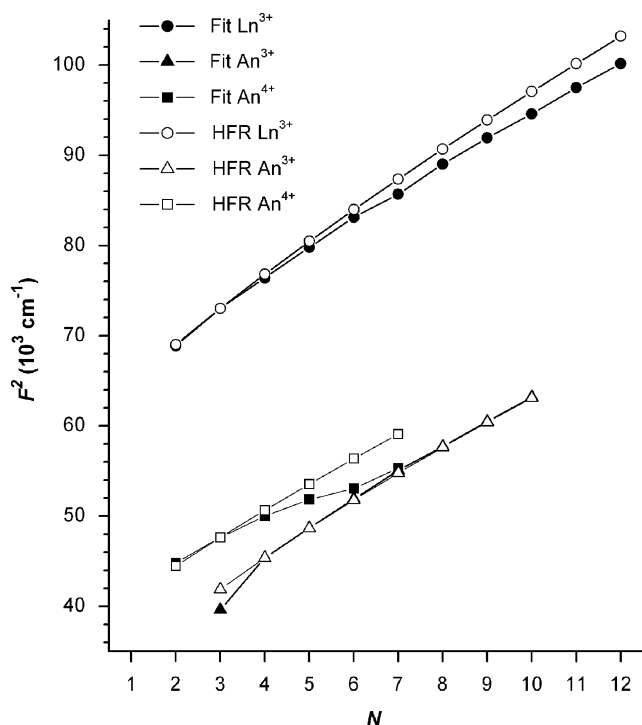
Fig. 1. Systematic variation of experimentally determined (fit) and relativistic Hartree-Fock (HFR) electrostatic interaction parameter F^2 as a function of number of f-electrons (N) for Ln^{3+} in LaF_3, and An^{3+} in $LaCl_3$, and An^{4+} in AnF_4. To normalize the data, the HFR values of F^2 are subtracted by $29702\,cm^{-1}$, $29562\,cm^{-1}$, and $32262\,cm^{-1}$, respectively, for the Ln^{3+} series, An^{3+} series, and An^{4+} series. For An^{3+}, except U^{3+}, the HFR and Fit values of F^2 agree very well so they are overlapped on each other and show no difference.

Fig. 2. Systematic variation of experimentally determined (fit) and Hartree-Fock (HFR) spin–orbit interaction parameter ζ as a function of number of f-electrons (N) for Ln^{3+} in LaF_3, and An^{3+} in $LaCl_3$, and An^{4+} in AnF_4. The HFR values of ζ are subtracted by $65\,cm^{-1}$, $272\,cm^{-1}$, and $376\,cm^{-1}$, respectively, for the Ln^{3+} series, An^{3+} series, and An^{4+} series. For An^{3+}, the HFR and Fit values of ζ_{5f} agree very well so they are overlapped on each other and show little difference.

on average to an approximately 5% change [6]. Because of the absence of mechanisms that absorb these effects in the HFR model, HFR values of F^ks cannot be used directly as initial parameters for the least squares fitting process. Scaling of HFR values to the experimentally determined ones is necessary to establish a systematic trend for a specific parameter. With this procedure, linear extrapolations of model parameters from one ion to another lead to values consistent with those obtained in the actual fitting process.

In addition to HFR calculations of F^ks and ζ_{nf}, estimated values for M^k, $k = 0, 2, 4$, can also be computed using the HFR method [23]. These parameters do not vary dramatically across the f-series. In practice, experience has shown that they can be taken as given or varied as a single parameter while maintaining the HFR ratios $M^2/M^0 = 0.56$ and $M^4/M^0 = 0.31$ [37]. For actinide ions, the ratio M^4/M^0 may be maintained at 0.38–0.4.

For the rest of the free-ion effective operators introduced above, no direct Hartree-Fock values can be derived. Only a term-by-term HFR calculation is possible to give additional guidance for parameter estimates. For example, the HFR values of P^ks for Pr^{2+} and Pr^{3+} have been determined by Copland et al.
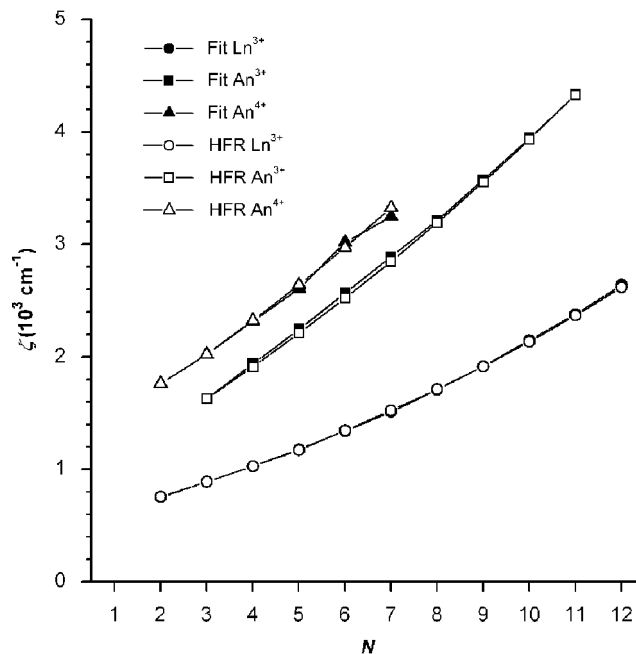
[38,39]. In establishing systematic trends of parameters for An^{3+}:$LaCl_3$, Carnall [37] constrained the P^k parameters by the ratios $P^4 = 0.5P^2$ and $P^6 = 0.1P^2$ while P^2 was varied freely along with other parameters. These ratios are consistent with the HFR estimation. The variation of these parameters across the series is not significant, and no obvious systematic trends have been established.

In fitting of experimental spectra, once the systematic trends of free-ion parameters are established, constraints can be imposed on other parameters that are relatively insensitive to the available experimental data. Some parameters such as T^i, M^k and P^k do not vary significantly across the series and to a good approximation have the same values for neighboring ions in the same series. In fact, in most of dielectric crystals the free-ion parameters are not host sensitive. Typically, there are approximately 1% changes in the values of the free-ion parameters between different lattice environments.

The significant reduction of slopes in the variation of F^k for An^{4+} compared to the HFR values, particularly for F^2 shown in Fig. 1 is consistent with the trends in the energy levels of An^{4+} which become increasingly similar to that for iso-f-electronic An^{3+} ions with increasing atomic number. The systematic deviation from the HFR values in free-ion electrostatic interaction for heavier An^{4+} provides rational for weakening f-electron

coupling and increasing ligand impact to the energy level structure of those ions.

It has been shown that a significant change in the ratios of F^4/F^2 and F^6/F^2 from U^{4+} to Np^{4+} is required in order to fit the experimental data [10,16]. However, in the analysis of the transneptunium ions, the ratios of F^4/F^2 and F^6/F^2 could be held constant. In this context, values of F^2 for all the ions studied exhibited a functional (but not linear) increase with atomic number. It is important to note that values of F^2 for all transneptunium members of the AnF_4 series would be poorly estimated based solely on linear projections from U^{4+} or Np^{4+}. Similar to the An^{3+} series, a regular behavior appears to be characteristic of the transneptunium actinide tetrafluorides. The computed values of ζ_{5f} from fitting the experimental data are generally quite consistent with the HFR values normalized to agree with the empirical value for NpF_4.

The parametric free-ion electrostatic interaction parameters F^k for UF_4 and NpF_4 are a few percent larger than those that have been determined by fitting spectroscopic data for the tetravalent chlorides and bromides, and those for UF_4 are smaller than the gaseous free-ion values for UV [40], as expected. Indeed all of the free-ion parameter values used in the analysis of AnF_4 spectra are fully consistent with those available from other analysis of An^{4+} spectra in a variety of crystal environments [17].

The difference in free-ion interaction parameters between the $4f$ ions and the $5f$ ions is expected due to the expansion of the electronic orbital. As a result, the electrostatic interaction should be reduced while spin–orbit coupling becomes much stronger. In combination, these two effects lead to a more compressed and LS-term mixed free-ion energy level structure. Fig. 3 gives the ratios of F^2_{5f}/F^2_{4f} and ζ_{5f}/ζ_{4f}. In average these ratios are approximately 0.6 and 1.9, respectively, for F^2_{5f}/F^2_{4f} and ζ_{5f}/ζ_{4f}. The values are from the systematic analyses of the crystal-field spectra for Ln^{3+}:$LaCl_3$ and An^{3+}:$LaCl_3$. Significant changes in the values and their ratios are not expected for the two series of f-elements in other crystalline hosts. However, because the strength of spin–orbit coupling has the same scale as the electrostatic interaction, intermediate coupling scheme must be used in evaluation of the crystal-field splitting.

2.2. Crystal-field strength: covalence vs. point charge contribution

In the literature, the overall effect of crystal-field interaction is often characterized by quantitative comparison of the crystal-field strength defined as [41]:

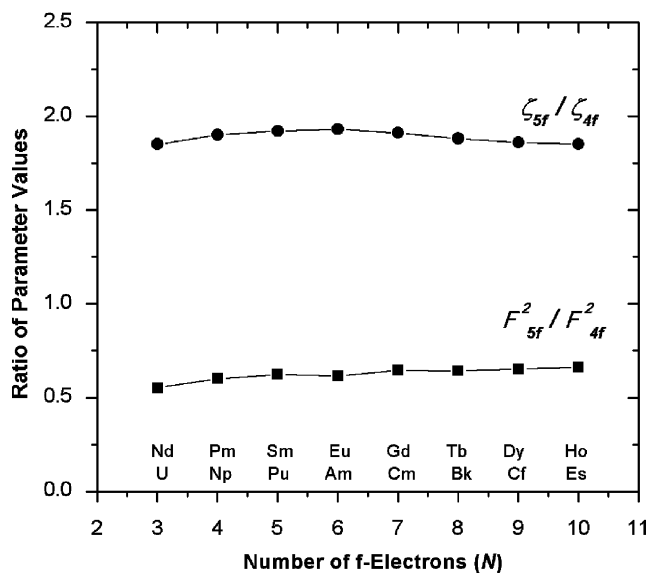$$N'_v = \left[\sum_{q,k} \frac{|B^k_q|^2}{2k+1} \right]^{1/2}. \tag{4}$$

Fig. 3. Systematic comparison of the free-ion interaction parameters between the trivalent lanthanide (4f) ions and the actinide (5f) ions in $LaCl_3$.

The values of crystal-field parameters and particularly the crystal-field strength characterize the integrated effect of ion–ligand interactions. However, this is only an average parameter with contributions from all crystal-field components. One should be aware of that for some crystal-field states, these contributions may mutually compensate. Based on the theory of crystal-field interaction, a greater insight can be gained into crystal-field analysis and energy level calculations. By defining ion–ligand interaction in terms of the static point charge interaction and exchange charge interaction, it is possible to evaluate contributions from the electrostatic crystal-field parameters and those from overlap and covalence effects. The ECM of crystal-field theory introduces a renormalization of the parameters of the electrostatic crystal field only and does not change the structure of the Hamiltonian.

The ECM [29,30,42] is an extension of the angular overlap model proposed by Jørgensen [43]. It separates point charge electrostatic coupling and spatial distribution of electron density. Instead of Eq. (3), the effective crystal field Hamiltonian is assumed to be a sum of two terms

$$\mathscr{H}_{CF} = \mathscr{H}^{pm} + \mathscr{H}^{ec}, \tag{5}$$

where the first term corresponds to the electrostatic interaction of valence electrons localized on the f-element ion with point multipole moments of lattice ions. The second term approximates all contributions due to the spatial distribution of electron density. Both terms have the form of Eq. (3) and are associated with parameters $B^{(pm)k}_q$ and $B^{(ec)k}_q$, respectively.

The renormalization of crystal-field Hamiltonian may be considered to be a result of the "nonlocal"

interaction of the valence electron with the exchange charges localized at the bonds connecting the metal ion with its nearest neighbor ions. Values of the exchange charges are proportional to the linear combinations of the overlap integrals and depend on the rank k of the corresponding tensor, namely, the crystal-field parameter $B^{(k)}$. The ECM allows for consideration of both even and odd components of the crystal field. In particular, integral intensities of spectral lines in the intraconfigurational $4f^N - 4f^N$ transitions for lanthanide (or $5f^N - 5f^N$ for actinide) spectra and their energies may be fitted in the framework of the empirical crystal-field modeling. For a comparison, Table 1 lists the values of crystal-field parameters for actinide and lanthanide ions calculated by using the ECM in comparison with the experimentally determined ones [44,45]. It is evident that the dominant contributions to B_q^2 are from electrostatic interactions, whereas those to B_q^4 and B_q^6 are from short-range interactions and are dominated by the exchange charge contribution. It is generally realized that the second-order parameters B_q^k with $k = 2$ are less accurately determined by the model calculation, particularly for a disordered lattice. This is because the second-order parameters characterize the long-range electrostatic interactions that are difficult to calculate accurately. It should be noted that the contradiction between the calculated and experimental values of the B_0^2 parameter in Nd^{3+}:LaCl$_3$ (in particular, different signs) may be removed when taking into account large contributions due to point dipole and quadrupole moments of the chlorine ions [46].

It is now realized that in average the crystal-field strength of actinide ions is approximately twice of that for lanthanide ions in the same hosts [13,15,47]. A general interpretation is that the radial distribution of the $5f$ orbital is more extended than that of the $4f$ orbital. Therefore, in comparison with the $4f$ electrons, the interaction between the $5f$ electrons and the ligand electrons is less shielded by the outer shell $7s$ and $7p$ electrons. As a result, actinide bonding has more contribution from orbital overlap and covalence. To elucidate the nature of ion–ligand interaction, let us compare the ratios of the crystal-field parameters of different ranks, namely, evaluating $r_{kq} = B_q^k(5f^N)/B_q^k(4f^N)$. These ratios for Ln^{3+}:LaCL$_3$ and An^{3+}:LaCl$_3$ are plotted in Fig. 4 as a function of N [6,11]. Except for the first pair of the f^3 (U^{3+}/Nd^{3+}) ions, it is quite
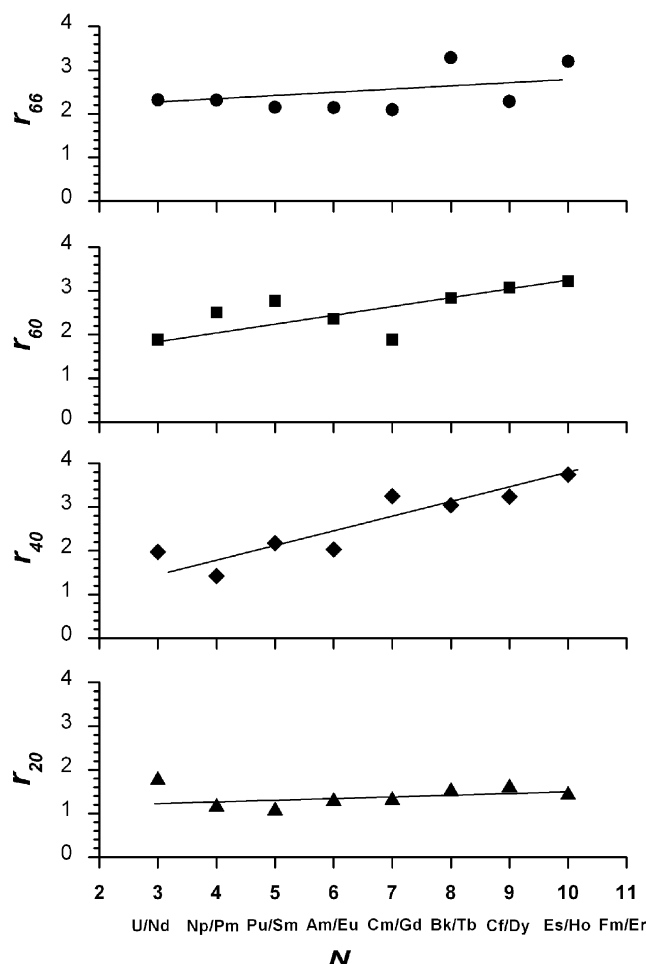

Fig. 4. Systematic comparison of the crystal-field interaction parameters between the trivalent lanthanide ($4f$) ions and the actinide ($5f$) ions in LaCl$_3$.

Table 1

Comparison of the calculated and experimentally determined (fit) values of the crystal-field parameters (cm^{-1})

	Nd^{3+}:LaCl$_3$ [44]			Am^{3+}:LaCl$_3$ [44]			Cm^{3+}:LuPO$_4$ [45]		
	B_q^k (tot)	B_q^k (EC)	B_q^k (fit)[a]	B_q^k (tot)	B_q^k (EC)	B_q^k (fit)[a]	B_q^k (tot)	B_q^k (EC)	B_q^k (fit)
B_0^2	−78	39	81	−41	81	121	450	180	399
B_0^4	−78	−57	−42	−197	−142	−73	370	230	363
B_4^4	—	—	—	—	—	—	2400	1200	2261
B_0^6	−44	−41	−44	−90	−80	−118	−2500	−2050	−2470
B_4^6	—	—	—	—	—	—	200	185	167
B_6^6	299	279	439	656	588	1066	—	—	—
B_{-6}^6	−239	−226	—	−515	−471	—	—	—	—

[a]For ions in LaCl$_3$, calculation was based on C_{3h} while fitting was to D_{3h} symmetry without B_{-6}^6.

consistent that r_{20} is approximately 1.2, whereas the ratios for the rank 4 and 6 crystal-field parameters are larger than 2.0. This result indicates that the rank 2 crystal-field parameters are of the same value for both lanthanide and actinide ions in the same lattice, however, the values of the rank 4 and 6 parameters are more than doubled. Same conclusion can be reached by comparing the crystal-field values for trivalent lanthanide and actinide ions in phosphates such as $LuPO_4$ and YPO_4 [13,14,45].

3. Correlation between crystal-field interaction and free-ion interaction

In empirical parameterization of the $4f$ crystal-field spectra, the variation of the electrostatic interaction parameters and the spin–orbit coupling parameter are less than 1% for the trivalent lanthanide ions in different hosts of ionic crystals. It was shown that the free-ion parameters established for Ln^{3+} in $LaCl_3$ do not change significantly when they are applied to analysis of spectra of Ln^{3+} in LaF_3 [5,6], and have been used successfully as the starting values in analyzing the crystal-field spectra of iso-f-electronic ions in other systems such as $LiYF_4$ [48]. Therefore, the correlation between the free-ion interaction and the crystal-field interaction for the $4f$ lanthanide ions is generally negligible. However, there are exceptions in which the patterns of the $4f^N$ energy level structure, namely the center of gravity of the J-multiplets, are sensitive to ligand environment, particularly for lanthanide ions in some inorganic crystals where there exist ion-ligand charge imbalance and require charge compensators [49,50]. For actinide ions in solids, the reduction in electrostatic interaction and increase in crystal-field interaction result in more significant influence of ligands to the electronic properties of the metal ion. The energy levels and electronic transition intensities are more strongly dependent on the surrounding local environment [11,13,16,17]. The increasing effect of crystal-field interaction thus reduces the influence of free-ion interaction.

3.1. Cm^{3+} systems

The diagonal matrix elements of crystal-field interaction are vanished for all f^7 states because of

$$\left\langle f^7 LS \left| C_q^{(k)} \right| f^7 LS \right\rangle = 0. \qquad (6)$$

As a result, the splitting and shift of the energy levels of a $4f^7$ (or $5f^7$) multiplet depend primarily on the spin–orbit coupling induced LS mixing and crystal-field induced J-mixing between different LS terms. While the intra ionic electrostatic interaction is still an important factor in determining the patterns of the energy level structure, the coupling of spin–orbit and the crystal-field interactions are the dominant mechanisms for the f^7

state crystal-field splitting. Specifically, the leading contribution is from the non-vanished second-order off-diagonal matrix elements such as

$$\Delta E \propto \sum_{L'S'} \sum_{k,q} \zeta B_q^K \left\langle LS \left| V^{(11)} \right| L'S' \right\rangle \left\langle L'S' \left| C_q^k \right| LS \right\rangle. \qquad (7)$$

In Eq. (7) we see that the spin–orbit coupling and crystal-field interaction have equivalent effects on the energy level splitting and shift in the center of gravity for a given J-multiplet. Spectroscopic studies of ions in such a configuration thus provide information unique for understanding f-element electronic interactions. Fig. 5 shows the correlation of the crystal-field strength N_v' with free-ion interaction parameters F^2 and ζ_{5f}, and the shift of the center of gravity for two multiplets of Cm^{3+} in $LaCl_3$ [51], $LuPO_4$ [45,52], $CsCdBr_3$ [53], Cs_2NaYCl_6 [54], and ThO_4 [55]. A trend is evident that the values of F^2 and ζ_{5f} and the center of gravities $E_{ave}(^6D'_{7/2})$ and $E_{ave}(^6P'_{5/2})$ decrease with increasing crystal-field strength, N_v'.

3.2. U^{4+} systems

For tetravalent actinide ions, it is useful to emphasize that the crystal field is no longer a small interaction relative to that of the free ion, but is capable of radically
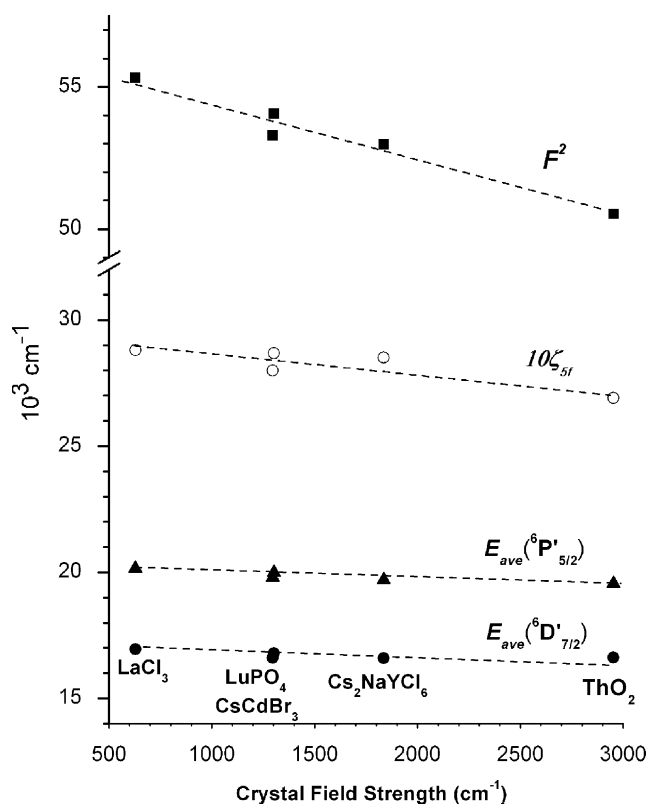

Fig. 5. Systematic correlation of the crystal-field strength (N_v') with the free-ion interaction parameters (F^2 and ζ_{5f}) and the center of gravities (E_{ave}) for Cm^{3+} in various crystals.

transforming the energy level scheme without any change in magnitude of the free-ion interaction parameters. This is readily evident in comparing the parameters and energy level schemes for UCl_4 and Cs_2UCl_6 [12,17,18]. One of the consequences of this change in the hierarchy of interactions that comprise the theoretical model is that there is a decreased sensitivity in energy level structure calculations to the values of the F^k integrals in the analysis of An^{4+} spectra compared to those of the An^{3+} and Ln^{3+} systems. This is a direct result of the stronger crystal-field and spin–orbit interactions. Understanding of this fact is important because it explains the relatively uncertain F^k values obtained from fitting experimental data. In most cases, very few free-ion states are actually included in the calculation. Indeed, those states that are included tend to be the lowest energy states in the configuration and to exhibit the smallest J mixing that would aid in defining the parameters.

In reviewing the previously reported free-ion and crystal-field parameters for tetravalent uranium in various crystals, we found that the trend of correlation between the crystal-field strength and the free-ion parameters is similar to that of Cm^{3+}. For U^{4+} doped, respectively, in crystals of Ba_2YCl_7 [56], $ThBr_4$ [57], UF_4 [10], $ZrSiO_4$ [17,18] and $CsUCl_6$ [58], the values of F^2 and ζ_{5f} are plotted in Fig. 6 in comparison with the variation of N_v'. Whereas the variation of F^2 and ζ_{5f} is less significant than that of N_v', the correlation and systematic trend are evident and consistent with that shown in Fig. 5 for the Cm^{3+} systems, namely, the values of F^2 and ζ_{5f} decrease with increasing crystal-field strength.
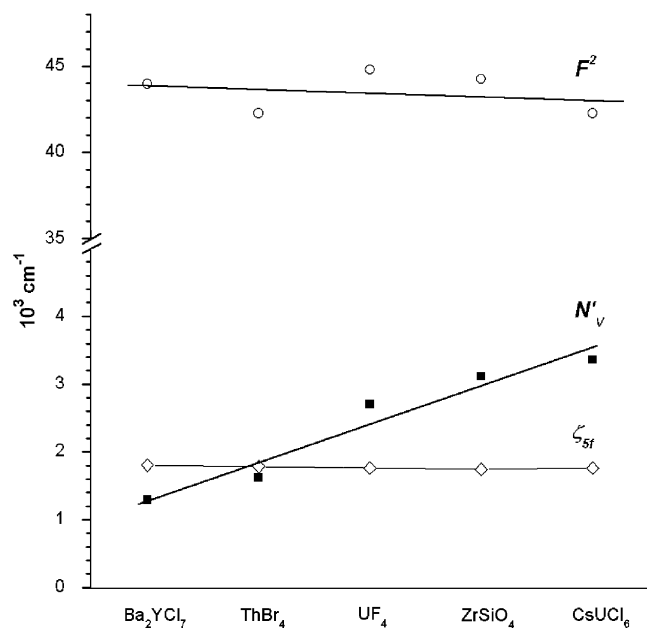

Fig. 6. Systematic correlation of the crystal-field strength (N_v') with the free-ion interaction parameters (F^2 and ζ_{5f}) for U^{4+} in various crystals.

4. Ground-state splitting of f^7 ions

As we mentioned in the previous section, ions in $4f^7$ ($5f^7$) configuration is of special spectroscopic properties. Particularly, interpretation of the crystal-field splitting of the nominal $^8S_{7/2}$ ground state in a half-filled shell of the f^7 configuration was contradictory in the history of f-element spectroscopy [14,51,59–62]. The lanthanides in such a configuration are Eu^{2+}, Gd^{3+}, and Tb^{4+}; and the actinide ions include Am^{2+}, Cm^{3+}, and Bk^{4+}. Early arguments were focused on the Gd^{3+} ion since that the ground-state crystal-field splitting observed in EPR experiments was less than $0.5\,cm^{-1}$ [63] and could not be interpreted satisfactorily by the crystal-field theory. A series of mechanisms were considered but failed to provide a consistent interpretation [62,64,65]. However, for the actinide ions, the $^8S_{7/2}$ ground-state splitting into four Kramers doublets is much larger than that of the Gd^{3+}. For Am^{2+} and Cm^{3+}, the observed splitting varies from 2 to $20\,cm^{-1}$ [14,51,52,66], while for Bk^{4+} it is on the order of $60\,cm^{-1}$ [16,59].

To summarize previous work, a comparison of the crystal-field splittings (four Kramers doublets) of Cm^{3+}, and Bk^{4+} ions in the ground-state is shown in Fig. 7 [45,51–55,59]. For the $5f^7$ systems, no additional mechanisms other than the crystal-field interaction are needed to provide a satisfactory interpretation to the observed splitting in the $^8S_{7/2}$ ground state of actinide ions [51,59]. The observed crystal-field splittings must be attributed to the contributions of the mixture of other LS terms into the ground state free-ion wavefunction and non-zero off-diagonal crystal-field matrix elements between these excited state LS terms. Because of the large energy gaps from the ground state to the excited multiplets of Gd^{3+}, the excited state LS components in the ground state is small, and J mixing is also negligible in this case. However, for the actinide ions in $5f^N$ configurations, the ground-state wave functions contains considerable LS components of the excited states, and thus lead to much larger splitting.

For the ground state of an f^7 configuration, all linear matrix elements of free-ion and crystal-field interactions are vanished. The lowest order non-zero matrix elements are the fourth-order coupling between the spin–orbit interaction and crystal-field interaction such as [67]

$$\langle ^8S|V^{(11)}|^6P\rangle\langle ^6P|C^{(2)}|^6D\rangle\langle ^6D|C^{(2)}|^6P\rangle\langle ^6P|V^{(11)}|^8S\rangle,$$
$$\langle ^8S|V^{(11)}|^6P\rangle\langle ^6P|C^{(4)}|^6G\rangle\langle ^6G|C^{(4)}|^6P\rangle\langle ^6P|V^{(11)}|^8S\rangle,$$
$$\langle ^8S|V^{(11)}|^6P\rangle\langle ^6P|C^{(6)}|^6I\rangle\langle ^6I|C^{(6)}|^6P\rangle\langle ^6P|V^{(11)}|^8S\rangle,$$
$$\langle ^8S|V^{(11)}|^6P\rangle\langle ^6P|V^{(11)}|^6D\rangle\langle ^6D|C^{(2)}|^6P\rangle\langle ^6P|V^{(11)}|^8S\rangle,$$

$$(8)$$

The ground state wavefunction in the intermediate coupling scheme varies significantly from Gd^{3+}, to Cm^{3+} and Bk^{4+}. In the framework of intermediate
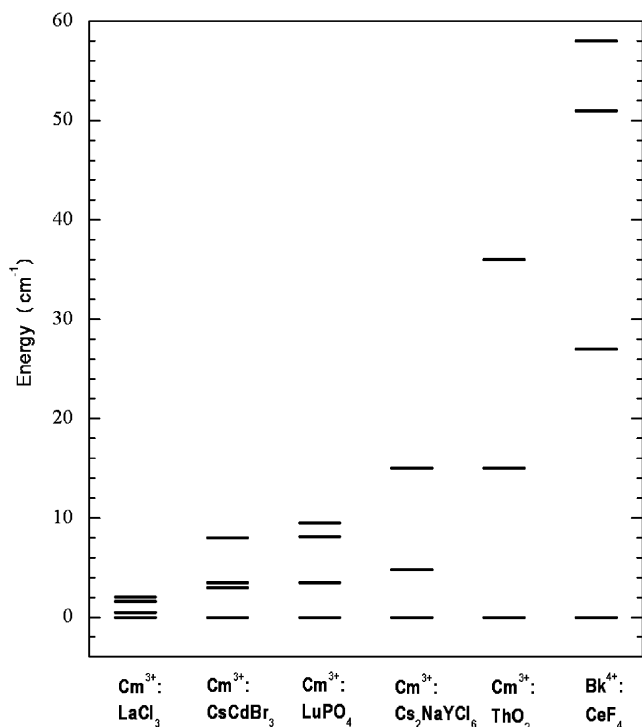
Fig. 7. Ground state splitting of Cm^{3+} in various crystals in comparison with that of Bk^{4+} in CeF_4.

Table 2
Dominant contribution to the ground state splitting of Cm^{3+} in Cs_2NaYCl_2 and ThO_2

	Cm^{3+}:Cs_2NaYCl_6 [54]	Cm^{3+}:ThO_2 [55]
B_0^4	4034	−6446
ΔE ($^8S_{7/2}$)	23	36
$|B_0^4|/\Delta E$	175	179

An analysis of crystal-field spectrum of Cm^{3+} in ThO_2 was reported by Thouvenot et al. [55]. The observed Cm^{3+} spectra are from the cubic lattice site and are assigned to phonon-assisted electric dipole transitions and to magnetic dipole transitions. From these assignments, the crystal-field parameters have been determined. The experimental energy levels for the ground term determined from the optical data and earlier ESR spectra are in good agreement with the calculated values. Similar work was performed on Cm^{3+}:Cs_2NaYCl_6 in octahedral (O_h) symmetry [54]. As an example to elucidate the relation between ground state splitting and crystal-field strength, we compare in Table 2 the relationship between the ground state crystal-field splitting and the values of B_0^4 for the two systems. Although the scale is significantly different, the ratio of B_0^4 and the total splitting of the ground state (ΔE) is about the same for these two systems, thus supports the crystal-field model and the argument that the ground state splitting in such a system is dominated by the exchange charge interaction.

5. Conclusions

After more than three decades of extensive studies on the spectroscopic properties of lanthanide ions and actinide ions in various crystalline hosts, and particularly, with information from systematic analysis of the optical spectra of f-element ions within the framework of crystal-field theory, a comprehensive analysis of systematic behaviors in free-ion and crystal-field interactions is now possible. We have interpreted the general trends in the variation of free-ion interaction parameters for lanthanide and actinide ions in various crystals and discussed several interesting phenomena in systematic properties of f-element crystal-field interaction. Comparison between the lanthanide series in $4f^N$ configuration and the actinide series in $5f^N$ configuration is useful for understanding the more extended $5f$-electronic interactions for actinide ions in solids. We have shown that through the systematic behaviors of two different systems that correlation between crystal-field interaction and free-ion interaction is evident in actinide systems. It is shown that increasing of crystal-field interaction results in a reduction in free-ion parameters F^k and ζ_{5f}. We have also shown that, through the systematic

coupling scheme, wavefunction of a free-ion state is obtained through diagonalization of the free-ion interaction Hamiltonian. Using the values of the free-ion parameters obtained previously in analysis of the crystal-field spectra, one can readily calculate the intermediate coupling wave function of an f-element ion. The wavefunctions of the ground state for Gd^{3+}, Cm^{3+}, and Bk^{4+} were tabulated by Brito and Liu [59]. For Gd^{3+}, the rank-2 (B_q^2) crystal-field matrix dominates the ground state splitting and the contribution from rank-4 (B_q^4) and rank-6 (B_q^6) crystal-field components are negligible. However, for Cm^{3+} and Bk^{4+}, the leading contribution is from the rank-4 (B_q^4) matrix and that from the rank-6 (B_q^6) is negligible.

Based on our previous discussion on the ECM of crystal-field theory, it is of interest in analysis of the crystal-field spectra of S-state ions in crystals of high symmetry, in which the rank-2 crystal-field matrix elements are vanished. For an f-element ion in a lattice of cubic symmetry, its crystal-field splitting depends only on B_0^4 and B_0^6. Based on the nature of the $5f$-ion crystal-field interaction, the ground state splitting of Cm^{3+} and Bk^{4+} should be dominated by the short-range exchange charge interaction. From the ground state wavefunction and non-zero matrix elements, we know that the B_0^6 has negligible contribution [59]. Therefore, for Cm^{3+} or Bk^{4+} in cubic lattice, contribution to the ground state splitting is primarily from the rank-4 crystal-field component, thus depends dominantly on B_0^4.

trends of Cm^{3+} and the U^{4+} systems, model calculations of crystal-field parameters in terms of exchange charge and static point charge contributions can provide a greater insight into the characteristics of ion-ligand interaction. Particularly, the extent of covalence in *f*-element compounds may be evaluated from analyses of crystal-field spectra. Finally, we should point out that the systematic trends established through empirical parameterization of the effective operator Hamiltonian and theoretical calculations based on ab initio methods or phenomenal crystal-field models in turn serve analyses of specific the *f*-element spectra and provide important information to characterization of chemical bonding and materials properties.

Acknowledgment

References

[1] B.G. Wybourne, Spectroscopic properties of rare earths, 1965.

[2] B.R. Judd, Operator Techniques in Atomic Spectroscopy, 1963.

[3] G.H. Dieke, Spectra and Energy Levels of Rare Earth Ions in Crystals, Wiley, New York, 1968.

[4] W.T. Carnall, P.R. Fields, K. Rajnak, J. Chem. Phys. 49 (1968) 4424.

[5] W.T. Carnall, G.L. Goodman, K. Rajnak, R.S. Rana, J. Chem. Phys. 90 (1989) 3443.

[6] H.M. Crosswhite, Systematic Atomic and Crystal-Field Parameters for Lanthanides in $LaCl_3$ and LaF_3, Colloq. Int. CNRS, 1976, Paris.

[7] H.M. Crosswhite, H. Crosswhite, J. Opt. Soc. Am B: Opt. Phys. 1 (1984) 246.

[8] C. Görller-Walrand, K. Binnemans, Rationalization of crystal-field parameterization. in: K.A. Gschneidner, J.A.L.E. (Ed.), Handbook on the Physics and Chemistry of Rare Earth, vol. 23. Elsevier, Amsterdam, 1996.

[9] S. Hüfner, Optical Spectra of Transparent Rare Earth Compounds, Academic Press, New York, 1978.

[10] W.T. Carnall, G.K. Liu, C.W. Williams, M.F. Reid, J. Chem. Phys. 95 (1991) 7194.

[11] W.T. Carnall, J. Chem. Phys. 96 (1992) 8713.

[12] W.T. Carnall, H.M. Crosswhite, Optical spectra and electronic structure of actinide ions in compounds and in solution. In: J.J. Katz, G.T. Seaborg, L.R. Morss (Eds.), The Chemistry of the Actinide Elements, vol. 2. 2nd ed. Chapman & Hall, London, 1986, pp. 1235.

[13] N.M. Edelstein, J. Alloys Compds. 223 (1995) 197.

[14] N. Edelstein, Proc. SPIE—Int. Soc. Opt. Eng. 4766 (2002) 8.

[15] G.K. Liu, Lanthanide and actinide optical spectra, In: D.J. Newman, A.B.N. (Eds.), Crystal Field Handbook. Cambridge University Press, Cambridge, 2000, pp. 65.

[16] G.K. Liu, W.T. Carnall, G. Jursich, C.W. Williams, J. Chem. Phys. 101 (1994) 8277.

[17] J.C. Krupa, Inorg. Chim. Acta 139 (1987) 223.

[18] J.C. Krupa, W.T. Carnall, J. Chem. Phys. 99 (1993) 8577.

[19] B.R. Judd, Proc. Phys. Soc. (London) 82 (1963) 874.

[20] B.R. Judd, Phys. Rev. 141 (1966) 4.

[21] H. Crosswhite, H.M. Crosswhite, B.R. Judd, Phys. Rev. 174 (1968) 89.

[22] J.E. Hansen, B.R. Judd, H. Crosswhite, Atomic Data Nucl. Data Tables 62 (1996) 1.

[23] B.R. Judd, H.M. Crosswhite, H. Crosswhite, Phys. Rev. 169 (1968) 130.

[24] W.T. Carnall, J.V. Beitz, H. Crosswhite, K. Rajnak, J.B. Mann, in: S.P. Sinha (Ed.), Systematics and the Properties of the Lanthanides, Reidel, Dordrecht, 1983, p. 389.

[25] W.T. Carnall, P.R. Fields, K. Rajnak, Energy levels and intensities in the solution absorption spectra of trivalent lanthanides, Argonne Nat. Lab., IL, USA. FIELD URL, 1968.

[26] W.T. Carnall, P.R. Fields, K. Rajnak, J. Chem. Phys. 49 (1968) 4412.

[27] W.T. Carnall, J. Less-Common Metals 122 (1986) 1.

[28] W.T. Carnall, NATO Advanced Study Institutes Series, Series C: Mathematical and Physical Sciences 44 (1979) 281.

[29] B.Z. Malkin, Z.I. Ivanenko, I.B. Aizenberg, Sov. Phys. -Solid State 12 (1970) 149.

[30] B.Z. Malkin, in: A.A. Kaplyanskii, R.M. Macfarlane (Eds.), Spectroscopy of Solids Containing Rare Earth Ions, North-Holland, Amsterdam, 1987, p. 13.

[31] D.J. Newman, Adv. Phys. 20 (1971) 197.

[32] D.J. Newman, B. Ng, J. Phys.: Condens. Matter 1 (1989) 1613.

[33] L. Seijo, Z. Barandiaran, J. Chem. Phys. 115 (2001) 55554.

[34] S. Matsika, Z. Zhang, S.R. Brozell, J.-P. Blaudeau, Q. Wang, R.M. Pitzer, J. Phys. Chem. A 105 (2001) 3825.

[35] H.M. Crosswhite, H. Crosswhite, J. Opt. Soc. Am. B 1 (1984) 246.

[36] W.T. Carnall, J.V. Beitz, H. Crosswhite, K. Rajnak, J.B. Mann, NATO ASI Series, Series C: Mathematical and Physical Sciences 109 (1983) 389.

[37] W.T. Carnall, A systematic analysis of the spectra of trivalent actinide chlorides in D3h site symmetry, Argonne Natl. Lab., Argonne, IL, USA, FIELD URL, 1989.

[38] G.M. Copland, D.J. Newman, C.D. Taylor, J. Phys. B: Atomic Molecular Phys. 4 (1971) 1388.

[39] G.M. Copland, D.J. Newman, C.D. Taylor, J. Phys. B: Atomic Molecular Phys. 4 (1971) 1605.

[40] C.H.H. Van Deurzen, K. Rajnak, J.G. Conway, J. Opt. Soc. Am. B 1 (1984) 45.

[41] F. Auzel, O.L. Malta, J. Phys. 44 (1983) 201.

[42] A.L. Larionov, B.Z. Malkin, Sov. Phys. Opt. Spectrosc. 39 (1975) 637.

[43] C.K. Jørgensen, Orbits in Atoms and Molecules, Academic Press, London, 1962.

[44] V.V. Zhorin, G.K. Liu, J. Alloys Compd. 275–277 (1998) 137.

[45] G.K. Liu, S.T. Li, V.V. Zhorin, C.-K. Loong, M.M. Abraham, L.A. Boatner, J. Chem. Phys. 109 (1998) 6800.

[46] M.V. Eremin, in: A.A. Kaplyanskii (Ed.), Spectroscopy of Crystals, Nauka, Leningrad, 1989.

[47] N. Edelstein, NATO ASI Series, Series C: Mathematical and Physical Sciences 155 (1985) 229.

[48] G.K. Liu, W.T. Carnall, R.P. Jones, R.L. Cone, J. Huang, J. Alloys Compd. 207–208 (1994) 69.

[49] J. Holsa, P. Porcher, J. Chem. Phys. 76 (1982) 2790.

[50] X.Y. Chen, G.K. Liu, J. Solid State Chem., 2004, this issue.

[51] G.K. Liu, J.V. Beitz, J. Huang, J. Chem. Phys. 99 (1993) 3304.

[52] K.M. Murdoch, N.M. Edelstein, L.A. Boatner, M.M. Abraham, J. Chem. Phys. 105 (1996) 2539.

[53] M. Illemassene, N.M. Edelstein, K.M. Murdoch, M. Karbowiak, R. Cavellec, S. Hubert, J. Lumin. 86 (2000) 45.

[54] K.M. Murdoch, R. Cavellec, E. Simoni, M. Karbowiak, S. Hubert, M. Illemassene, N.M. Edelstein, J. Chem. Phys. 108 (1998) 6353.

[55] P. Thouvenot, S. Hubert, N. Edelstein, Phys. Rev. B: Condens. Matter Mater. Phys. 50 (1994) 9715.

[56] M. Karbowiak, A. Mech, J. Drozdzynski, Phys. Rev. B 67 (2003) 195108.

[57] P. Delamoye, J.C. Krupa, J.G. Conway, N. Edelstein, Phys. Rev. B: Condens. Matter Mater. Phys. 28 (1983) 4913.

[58] D.R. Johnston, R.A. Satten, C.L. Schreiber, E.Y. Wong, J. Chem. Phys. 44 (1966) 3141.

[59] H.F. Brito, G.K. Liu, J. Chem. Phys. (2000) 4334.

[60] D.J. Newman, Australian J. Phys. 29 (1976) 177.

[61] D.J. Newman, W. Urban, J. Phys. C: Solid State Phys. 5 (1972) 3101.

[62] B.G. Wybourne, Phys. Rev. 148 (1966) 317.

[63] S. Hubert, J. Emery, N. Edelstein, J.C. Fayet, Solid State Commun. 54 (1985) 1085.

[64] D.J. Newman, J. Phys. C: Solid State Phys. 8 (1975) 1862.

[65] D.J. Newman, Chem. Phys. Lett. 6 (1970) 288.

[66] N. Edelstein, W. Easley, Zh. Eksp. Teor. Fiz. 48 (1968) 2110.

[67] C.W. Nielson, G.F. Koster, Spectroscopic Coefficeints for the pn, dn, and fn Configurations, The MIT Press, Cambridge, 1963.